Article

TRANSPARENT PROCESS

THE EMBO JOURNAL

Convergent regulation of the lysosomal two-pore channel-2 by Mg^{2+}, NAADP, $PI(3,5)P_2$ and multiple protein kinases

Archana Jha[1], Malini Ahuja[1], Sandip Patel[2], Eugen Brailoiu[3,*] & Shmuel Muallem[1,**]

Abstract

Lysosomal Ca^{2+} homeostasis is implicated in disease and controls many lysosomal functions. A key in understanding lysosomal Ca^{2+} signaling was the discovery of the two-pore channels (TPCs) and their potential activation by NAADP. Recent work concluded that the TPCs function as a $PI(3,5)P_2$ activated channels regulated by mTORC1, but not by NAADP. Here, we identified Mg^{2+} and the MAPKs, JNK and P38 as novel regulators of TPC2. Cytoplasmic Mg^{2+} specifically inhibited TPC2 outward current, whereas lysosomal Mg^{2+} partially inhibited both outward and inward currents in a lysosomal lumen pH-dependent manner. Under controlled Mg^{2+}, TPC2 is readily activated by NAADP with channel properties identical to those in response to $PI(3,5)P_2$. Moreover, TPC2 is robustly regulated by P38 and JNK. Notably, NAADP-mediated Ca^{2+} release in intact cells is regulated by Mg^{2+}, $PI(3,5)P_2$, and P38/JNK kinases, thus paralleling regulation of TPC2 currents. Our data affirm a key role for TPC2 in NAADP-mediated Ca^{2+} signaling and link this pathway to Mg^{2+} homeostasis and MAP kinases, pointing to roles for lysosomal Ca^{2+} in cell growth, inflammation and cancer.

Keywords channel; lysosome; Mg^{2+}; NAADP; TPC2
Subject Categories Membrane & Intracellular Transport
DOI 10.1002/embj.201387035 | Received 30 September 2013 | Revised 3 December 2013 | Accepted 5 December 2013 | Published online 2 February 2014
EMBO Journal (2014) 33, 501–511

Introduction

The pleiotropic effects of Ca^{2+} dictates highly compartmentalized and regulated cellular Ca^{2+} pools. Ca^{2+} is stored and released by several organelles, including the ER, mitochondria (Kiselyov *et al*, 2006; Clapham, 2007), and most notably the acidic endolysosomes (Galione & Ruas, 2005; Patel *et al*, 2010; Morgan *et al*, 2011; Patel & Muallem, 2011). In addition to regulating several endolysosomal functions, such as apoptosis (Kroemer *et al*, 2010), trafficking (Saftig & Klumperman, 2009), energy metabolism (Jewell *et al*, 2013) and fusion/fission events (Kiselyov *et al*, 2012), endolysosomal Ca^{2+} serves as a trigger that sensitizes Ca^{2+} release by neighboring IP_3 (Morgan *et al*, 2013) and ryanodine (Kinnear *et al*, 2004) receptors, possibly at membrane contact sites (Kilpatrick *et al*, 2013). Thus, understanding endolysosomal Ca^{2+} homeostasis is central to understanding endolysosomal function and cellular Ca^{2+} homeostasis.

At present, lysosomal Ca^{2+} homeostasis is poorly understood. Although it is established that lysosomal Ca^{2+} uptake depends on the lysosomal H^+ gradient, the transporter(s) coupling H^+ and Ca^{2+} transport is not known. The mechanism of Ca^{2+} release from the lysosomes is being studied more extensively since the seminal discoveries of the potent second messenger NAADP (Lee & Aarhus, 1995) and its ability to release Ca^{2+} from lysosomes (Churchill *et al*, 2002). Subsequently, the action of NAADP has been demonstrated in virtually all cell types examined and shown to mediate several lysosomal-related functions (Guse & Lee, 2008).

The identity of the channel activated by NAADP remains controversial. The major Ca^{2+}-permeable channels localized to the lysosomes are TRPML1 (Kiselyov *et al*, 2005; Pryor *et al*, 2006) and two pore channel TPC2 (Brailoiu *et al*, 2009; Calcraft *et al*, 2009). Although when activated pharmacologically, TRPML1 releases Ca^{2+} from an acidic compartment (Shen *et al*, 2012) consistent with its identity as the NAADP-activated channel (Zhang *et al*, 2011), other studies have ruled out its role in NAADP signaling (Yamaguchi *et al*, 2011). A breakthrough was made with the discovery of Two Pore channels (TPCs) as the more likely NAADP targets (Brailoiu *et al*, 2009; Calcraft *et al*, 2009; Zong *et al*, 2009). This is based on: (i) loss of response to NAADP in cells in which TPC expression was knocked-down with RNA interference (Brailoiu *et al*, 2009; Calcraft *et al*, 2009; Dionisio *et al*, 2011) and cells expressing channel-dead dominant-negative (DN) TPCs (Brailoiu *et al*, 2009; Pereira *et al*, 2011), (ii) a large increase in Ca^{2+} release and higher apparent affinity for NAADP in cells transfected with TPC1 or TPC2 (Brailoiu *et al*, 2009, 2010; Pereira *et al*, 2011; Yamaguchi *et al*, 2011), (iii) activation of

1 Epithelial Signaling and Transport Section, Molecular Physiology and Therapeutics Branch, NIDCR, NIH, Bethesda, MD, USA
2 Department of Cell and Developmental Biology, University College London, London, UK
3 The Department of Pharmacology, Temple University School of Medicine, Philadelphia, PA, USA
*Corresponding author. Tel: 215 707 2791; Fax: 215 707 9890; E-mail: ebrailou@temple.edu
**Corresponding author. Tel: 301 4020262; Fax: 301 4021228; E-mail: shmuel.muallem@nih.gov

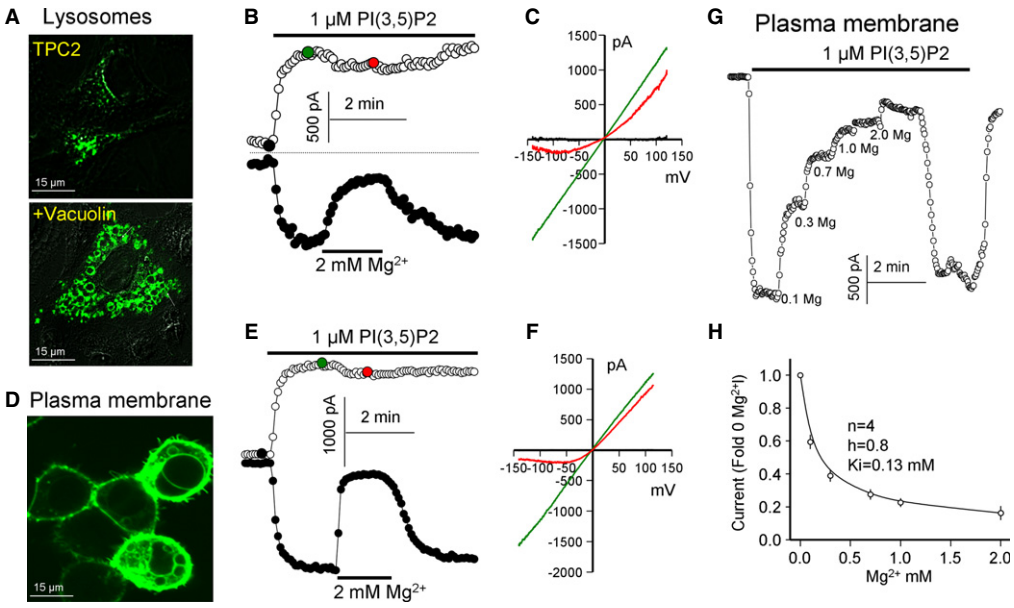

Figure 1. Regulation of $PI(3,5)P_2$-activated TPC2 current by Mg^{2+}_{cyt}.

A The images show localization of TPC2-GFP expressed in COS-7 cells with the lower cell treated with 1 μM vacuolin for 1 h.

B, C TPC2 current measured in enlarged lysosome extracted from COS-7 cell treated with vacuolin. At the time indicated by the bar, the lysosome was exposed to 1 μM of water-soluble $PI(3,5)P_2$ analogue, which activated TPC2. After maximal TPC2 current activation, the lysosome was exposed to 2 mM Mg^{2+}_{cyt}. (C) shows the I/V at the time indicated by the filled circles in (B). The mean ± s.e.m. is given in the text.

D An image of HEK cells transfected with the plasma membrane (PM)-targeted GFP-$TPC2^{L11L12/AA}$ mutant. Note the presence of TPC2-expressing vesicles attached to the PM in the cells expressing high level of TPC2. These cells were used for most experiments with excised PM patches since patches from these cells responded to NAADP.

E, F Excised PM patch expressing TPC2 was activated by 1 μM $PI(3,5)P_2$ and inhibited by 2 mM Mg^{2+}_{cyt}. (F) shows the I/Vs at the times indicated in (E) by the filled circles.

G TPC2 in a PM patch was activated by 1 μM $PI(3,5)P_2$. After maximal current activation the bath (cytoplasmic face) was perfused with solutions containing the indicated concentrations of Mg^{2+}.

H Mg^{2+}_{cyt} dependence of TPC2 inhibition. The results were fitted by a Hill equation and the fitted parameters are listed in the figure.

ion currents by NAADP in bilayers reconstituted with TPC1 (Rybalchenko *et al*, 2012), TPC2 (Pitt *et al*, 2010; Schieder *et al*, 2010) and plasma membrane (PM) patches obtained from cells expressing PM-targeted TPC2 (Brailoiu *et al*, 2010) and (iv) most notably, elimination of the response to NAADP in cells from TPC2 knockout mice (Calcraft *et al*, 2009; Tugba Durlu-Kandilci *et al*, 2010).

Nevertheless, two recent studies challenged a role of the TPCs in NAADP-mediated Ca^{2+} release. The first study reported that TPCs functions as a Na^+-selective channels that are activated by the endolysosomal phospholipid phosphatidylinositol-3,5-bisphosphate ($PI(3,5)P_2$) (Wang *et al*, 2012). Recording TPC2 channel activity in lysosomes enlarged by treatment with vacuolin or TPC2 targeted to the PM, the authors failed to activate the channel by NAADP. In addition, in cells from a TPC1 and TPC2 double knockout mouse line, Ca^{2+} release by NAADP remained intact, while the $PI(3,5)P_2$-activated Na^+ current was inhibited. In the second study, it was reported that the $PI(3,5)P_2$-activated TPCs currents are inhibited by the mTORC1 kinase complex (Cang *et al*, 2013).

The unexpected finding that the TPCs may not function in the NAADP response in spite of the numerous studies linking TPCs to NAADP, prompted us to re-examine the properties and regulation of TPC2. We show that TPC2 is activated by $PI(3,5)P_2$ and is Na^+-permeable. We discovered profound regulation of TPC2 by Mg^{2+} ions whereby cytosolic Mg^{2+} selectively inhibits TPC2 outward current while lysosomal Mg^{2+} modestly inhibits both the outward and inward currents. In the absence of Mg^{2+}, NAADP readily activates TPC2, with properties similar to $PI(3,5)P_2$. Further, we report novel regulation of TPC2 by P38 and JNK kinases. Notably, changes in $PI(3,5)P_2$, Mg^{2+} and the activity of JNK and P38 kinases function modified NAADP-mediated Ca^{2+} release similar to their effect on TPC2 current. These findings help to resolve conflicting views regarding activation of TPCs and its role in lysosomal Ca^{2+} signaling and reveal novel regulatory modes of major relevance to lysosome function.

Results

Regulation of TPC2 by Mg^{2+}

TPC2 was reported to function as a $PI(3,5)P_2$-activated channel when in lysosomes enlarged by vacuolin treatment to facilitate electrophysiological recording (Wang *et al*, 2012). We adopted the same approach to characterize the properties of TPC2. Fig 1A shows the effect of vacuolin on the subcellular distribution of TPC2-GFP expressed in COS7 cells. Mechanical release of the enlarged lyso-

somes and recording of whole lysosomal current using symmetrical Na^+ solutions confirmed activation of a TPC2-mediated Na^+ current by $PI(3,5)P_2$ (Fig 1B). During the course of our studies, we noted that TPC2 is strongly inhibited by cytoplasmic Mg^{2+} ($Mg^{2+}{}_{cyt}$). Intriguingly, $Mg^{2+}{}_{cyt}$ predominantly inhibited outward currents (Na^+ flowing from the cytoplasm into the lysosome, see Bertl *et al*, 1992 for definition) (Fig 1B and C). At 2 mM, $Mg^{2+}{}_{cyt}$ inhibited the $PI(3,5)P_2$-activated outward current by 74 ± 11% and the inward current by 23 ± 7% ($n = 6$). To independently confirm these results we re-routed TPC2 to the PM by mutation of a lysosomal, targeting sequence in $TPC2^{L11L12/AA}$ (Fig 1D). In cells expressing high levels of the mutant channel, it was present either predominantly in the plasma membrane (PM) or in both the PM and attached large vesicular structures. Patches excised from the two cell types showed the same Na^+ current, although the current from the cells containing the vesicular structures was higher. $Mg^{2+}{}_{cyt}$ preferentially inhibited $PI(3,5)P_2$-mediated TPC2 outward currents in PM patches (Fig 1E and F). Inhibition was concentration-dependent (Fig 1G) and was fitted well by a single exponential equation with a Hill coefficient of 0.8 and an apparent affinity for $Mg^{2+}{}_{cyt}$ of 0.13 mM (Fig 1H), well within the physiological range of free $Mg^{2+}{}_{cyt}$ of 0.2–0.5 mM (Gunther, 2006).

To further investigate the effects of Mg^{2+}, we examined whether TPC2 is regulated by luminal Mg^{2+} ($Mg^{2+}{}_{lys}$). At 2 mM $Mg^{2+}{}_{lys}$, both outward and inward $PI(3,5)P_2$-mediated currents in excised PM patches were reduced equally by about 50% (Fig 2A–C). $Mg^{2+}{}_{cyt}$ still specifically inhibited the residual outward current (Fig 2A–C). Since the lysosomal lumen is acidic, we also tested the effect of lysosomal pH (pH_{lys}) on the inhibition by $Mg^{2+}{}_{lys}$ and $Mg^{2+}{}_{cyt}$. Reducing pH_{lys} to 6.5 had no effect on the extent of the current (Fig 2A and D), the shape of the I/V curves (Supplementary Fig S1) or the Na^+/K^+ selectivity (Fig 2D). However, under these conditions, inhibition by $Mg^{2+}{}_{lys}$ was completely relieved whereas inhibition by $Mg^{2+}{}_{cyt}$ was unaffected (Fig 2E and F). Together, data in Figs 1 and 2 reveal a novel role for Mg^{2+} in regulating TPC2 activity.

TPC2 is regulated by NAADP in a Mg^{2+}-sensitive manner

In light of conflicting reports regarding the sensitivity of TPCs to NAADP and the inhibitory effects of Mg^{2+} on TPC activity reported here, we re-examined the effects of NAADP on TPC2 activity. Importantly, we demonstrate using three experimental paradigms that NAADP activates a current similar to $PI(3,5)P_2$.

First, in 42 out of 44 lysosome recordings from six independent transfections, NAADP (100 nM) evoked a Na^+ current (Fig 3A). A higher concentration of NAADP (1 μM), also evoked a current but in 8 out of 20 experiments the responses were transient (Supplementary Fig S3A), perhaps indicative of desensitization (Aarhus *et al*, 1996; Genazzani *et al*, 1996). When the current was sustained, channel activity was lost upon washout of NAADP

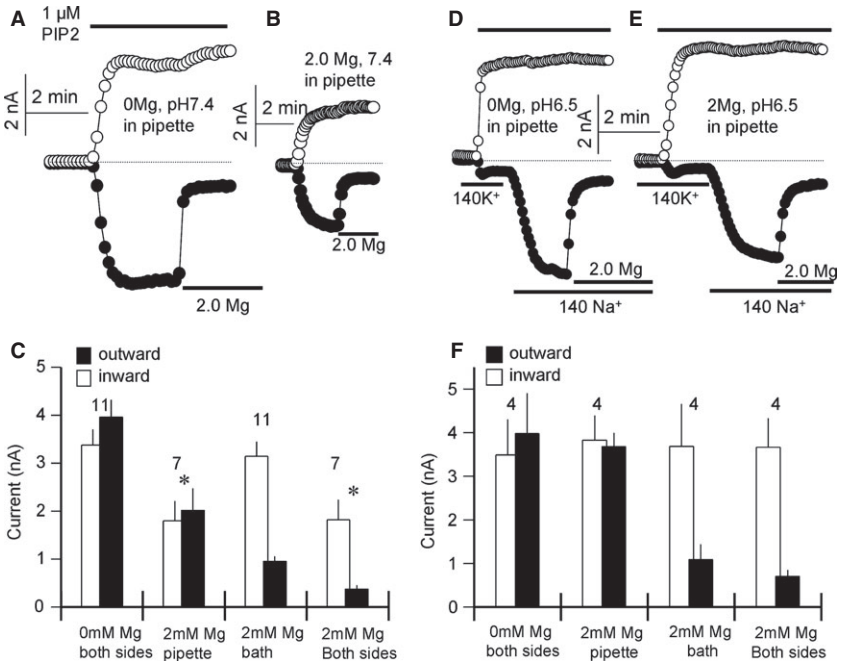

Figure 2. Regulation of $PI(3,5)P_2$-activated TPC2 current by $Mg^{2+}{}_{lys}$ and pH_{lys}.

All experiments were with excised patches from HEK cells expressing TPC2.

A, B, D, E The pipette solution (equivalent to lysosomal lumen) was Mg^{2+}-free, pH 7.4 in (A), contained 2 mM Mg^{2+}, pH 7.4 in (B), was Mg^{2+}-free, pH 6.5 in (D) and contained 2 mM Mg^{2+}, pH 6.5 in (E). In all experiments TPC2 was activated by 1 μM $PI(3,5)P_2$ and after maximal activation of the current the patches were exposed to a bath solution containing 2 mM Mg^{2+} to assay inhibition by $Mg^{2+}{}_{cyt}$. In (D, E) the experiments started with bath solution containing 140 mM K^+ that was then replaced with solutions containing 140 mM Na^+.

C Summary of the indicated number of experiments similar to those in (A, B).

F Summary of the indicated number of experiments similar to those in (D, E) * denotes $P < 0.05$ for the outward current relative to 0 mM Mg^{2+}, pH 7.4 pipette conditions as in (A).

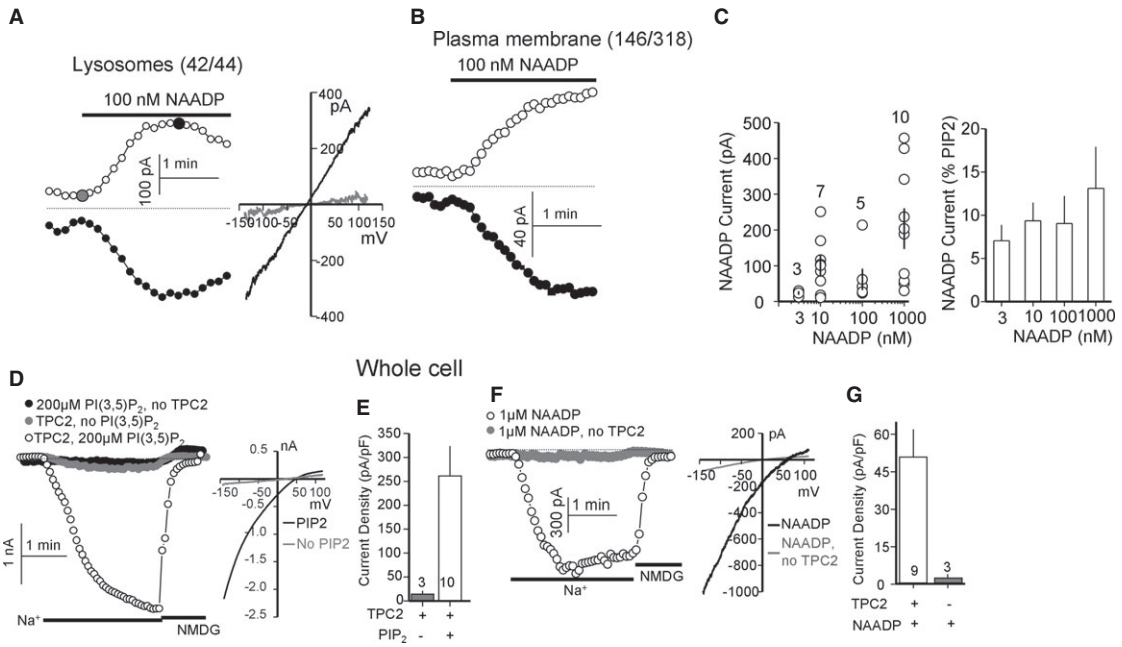

Figure 3. Activation of TPC2 by NAADP.

A Lysosomes expressing TPC2 were stimulated with 100 nM NAADP. The I/V at the times indicated by the closed circles. Activation by NAADP was observed in 42 out of 44 lysosomes.

B PM patches expressing TPC2 were stimulated with 100 nM NAADP. Current activation was observed in 146/318 patches.

C Excised PM patches were used to determine the dose response for activation of TPC2 by NAADP. The individual currents are shown in the scatter plot (left panel) and the averaged currents normalized to the current activated by $PI(3,5)P_2$ is shown in the columns (right panel).

D, E The whole-cell Na^+ current was measured in non-transfected HEK cells infused with 200 μM $PI(3,5)P_2$ (●) or HEK cells expressing TPC2 and infused with buffer (◉) or 200 μM $PI(3,5)P_2$ (○). (E) shows the mean ± s.e.m. of the indicated number of experiments similar to those in (D).

F, G The whole-cell Na^+ current was measured upon infusion of either non-transfected (◉) or TPC2-expressing (○) cells with 1 μM NAADP. (G) shows the mean ± s.e.m. of the indicated number of experiments similar to those in (F).

(Supplementary Fig S3B). Second, NAADP-mediated channel activity could also be recorded in PM patches (Fig 3D). The success rate was lower (146/318) and activation by NAADP was observed mostly in cells expressing high levels of $TPC2^{L11L12/AA}$ (Fig 1D). The excised patches were used to determine the dependence of the current on NAADP concentration. Variability of the current (Fig 3C, left panel) precluded accurate determination, although when normalized to the current activated by $PI(3,5)P_2$ in the same patches, the current could be activated by as low as 3 nM NAADP (Fig 3C, right panel), consistent with the high affinity for activation of Ca^{2+} release by NAADP (Galione & Ruas, 2005; Patel *et al*, 2010). The difference between the currents activated by the indicated NAADP concentrations did not reach statistical significance and for 3/10 nM, 3/1 μM, and 10/1 μM it was between $P = 0.09–0.13$. The magnitude of the currents however were only approximately 10% of those evoked by $PI(3,5)P_2$ (Fig 3C).Third, infusion of NAADP (1 μM) evoked a Na^+ current in whole cell recording (Fig 3F and G) similar to $PI(3,5)P_2$ (Fig 3D and E).

Importantly, NAADP-evoked currents were regulated by Mg^{2+} independently of the experimental method used. Thus, the outward lysosomal current was inhibited by $Mg^{2+}{}_{cyt}$ (100%, $n = 4$; Fig 4A) and selective for Na^+ over K^+ (Fig 4B and C). NAADP-mediated currents in excised PM patches were also blocked by $Mg^{2+}{}_{cyt}$ with an apparent affinity of 60 μM (Fig 4D and E). However, this value is less reliable than that obtained with $PI(3,5)P_2$ (Fig 1) due to the small and variable current. Finally, whole-cell currents in response to both NAADP and $PI(3,5)P_2$ were also Mg^{2+}-sensitive (Supplementary Fig S2). Intracellular Mg^{2+} (equivalent to $Mg^{2+}{}_{cyt}$) inhibited the outward current by more than 98% and the inward current by about 20% (Supplementary Fig S2A and B). Extracellular Mg^{2+} (equivalent to $Mg^{2+}{}_{lys}$) inhibited both currents by about 20% (Supplementary Fig S2C and D). We noted that in these recordings, the outward current was smaller than the inward current. The reason for this is not clear at the present time but may reflect channel regulation that is not observed in excised patches or isolated lysosomes. Nevertheless, regulation by Mg^{2+} is clearly evident. Taken together, these findings show that under defined ionic conditions, TPC2 can be readily activated by both NAADP and $PI(3,5)P_2$.

TPC2 is regulated by multiple protein kinases

A recent study showed that the mTORC1 kinase complex inhibits TPC2 activity (Cang *et al*, 2013). In accord, we found that in lysosomes expressing TPC2 and PM patches expressing $TPC2^{AA}$, MgATP induced a time-dependent inhibition of $PI(3,5)P_2$ currents (Supplementary Fig S4). This effect was slowed by chemical (rapamycin) and molecular (overexpression of DN mTORC1) inhibition of mTORC1 but unaffected by overexpression of wild-type mTORC1 (Supplementary Fig S4). The relatively modest effect of mTORC1 manipulation on the inhibitory effects of MgATP prompted us to

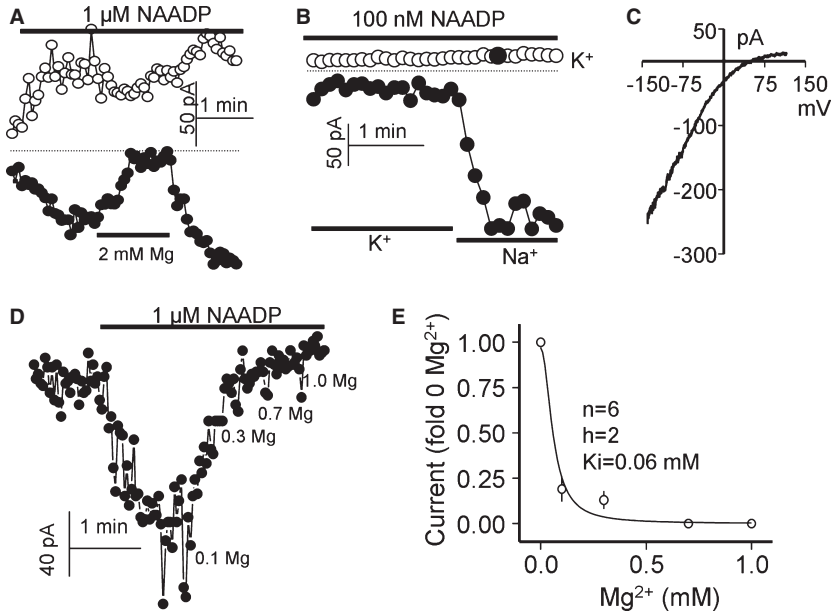

Figure 4. Selectivity and Mg^{2+}_{cyt} dependence of the NAADP-activated TPC2 current.

A Lysosomes expressing TPC2 were stimulated with 1 μM NAADP and then exposed to 2 mM Mg^{2+}, which completely inhibited the outward and partially the inward currents.

B, C TPC2 current in endolysosomes activated by NAADP is highly Na^+/K^+-selective. (C) shows the I/Vs at the time indicated by the closed circle in the upper symbols.

D, E Shows the Mg^{2+}_{cyt} dependence of the NAADP-activated TPC2 current in endolysosomes. The results in (E) were fitted with a Hill equation and the parameters are listed in the Figure.

explore the role of other protein kinases in regulating TPC2 activity. We focused on MAP kinases given their established roles in regulating lysosomal functions such as apoptosis, autophagy and energy metabolism (Wagner & Nebreda, 2009; Settembre *et al*, 2013). In an initial screen using MAP kinase inhibitors at concentrations five times the reported IC_{50}, blockade of MAP2K and MEKs had no effect of the rate or extent of TPC2 inhibition by MgATP. Inhibition of the MgATP response was observed with the inhibitors of JNK and P38 and was thus characterized in detail.

The effect of the kinases was evaluated both in lysosomes and PM patches. The JNK inhibitor SP600125 (SP60) markedly delayed inhibition of TPC2 currents by MgATP in lysosomes (Fig 5A) and PM patches (Fig 5C). A summary of pooled data quantifying the extent and time constants for inhibition by MgATP under the various conditions is provided in Fig 5B and D. Importantly, expression of DN-JNK strongly suppressed inhibition whereas expressing wild-type JNK had the opposite effect (Fig 5A and C). In PM patches from cells overexpressing high levels of JNK, $PI(3,5)P_2$-mediated currents in the absence of MgATP were substantially lower than in control cells presumably reflecting phosphorylation of TPC2 in intact cells. Consistent with this notion, pre-treating cells with 0.4 μM SP60 prior to recording of $PI(3,5)P_2$-mediated currents reversed the inhibitory effects of JNK overexpression (Supplementary Fig S5A and B). These data reveal a novel role for JNK in regulating TPC2.

Similar experiments manipulating P38 activity are shown in Fig 6. As with JNK, chemical inhibition of P38 with 1.5 μM SB202190 (SB20) or overexpression of DN-P38 suppressed inhibition of $PI(3,5)P_2$ currents by MgATP. When TPC2 was targeted to the PM, expression of P38 strongly inhibited the current in the absence of MgATP even when it was transfected at low levels (0.2 μg/ml). The inhibition was reversed by inhibition of P38 with SB20 (Supplementary Fig S5B). In experiments in which the current was inhibited by only about 50% by P38, it accelerated the inhibition of TPC2 by MgATP (normalized green trace in Fig 6C, and summary in D). Together, the results in Figs 5 and 6 and Supplementary Fig S4 indicate that TPC2 function is regulated by multiple protein kinases.

Regulation of the NAADP-mediated Ca^{2+} signals by $PI(3,5)P_2$, Mg^{2+} and protein kinases

To determine the physiological significance of the present findings in intact cells and determine whether TPC2 currents and Ca^{2+} mobilizing activity of NAADP are related, we examined the effect of manipulating $PI(3,5)P_2$, Mg^{2+}, JNK and P38 levels on NAADP-mediated Ca^{2+} release. Fig 7A and B show that inhibition of $PI(3,5)P_2$ synthesis by YM201636 (an inhibitor of the organellar PI3P kinase PIKfyve) inhibited endogenous NAADP-mediated Ca^{2+} signals in SKBR3 cells (Fig 7A). YM201636 also inhibited NAADP responses in cells transfected with TPC2 (Fig 7B). Conversely, increasing endolysosomal $PI(3,5)P_2$ by expression of PIKfyve (Ho *et al*, 2012) increased the extent and duration of endogenous NAADP-evoked Ca^{2+} signals (Fig 7A). Increasing cytoplasmic Mg^{2+} to between about 0.3–1 mM dose-dependently inhibited the response to NAADP (Fig 7C). Notably, expression of the JNK and P38 kinases also inhibited, while expression of dominant-negative JNK or P38 increased the extent and duration of the NAADP-mediated Ca^{2+} release (Fig 7D).

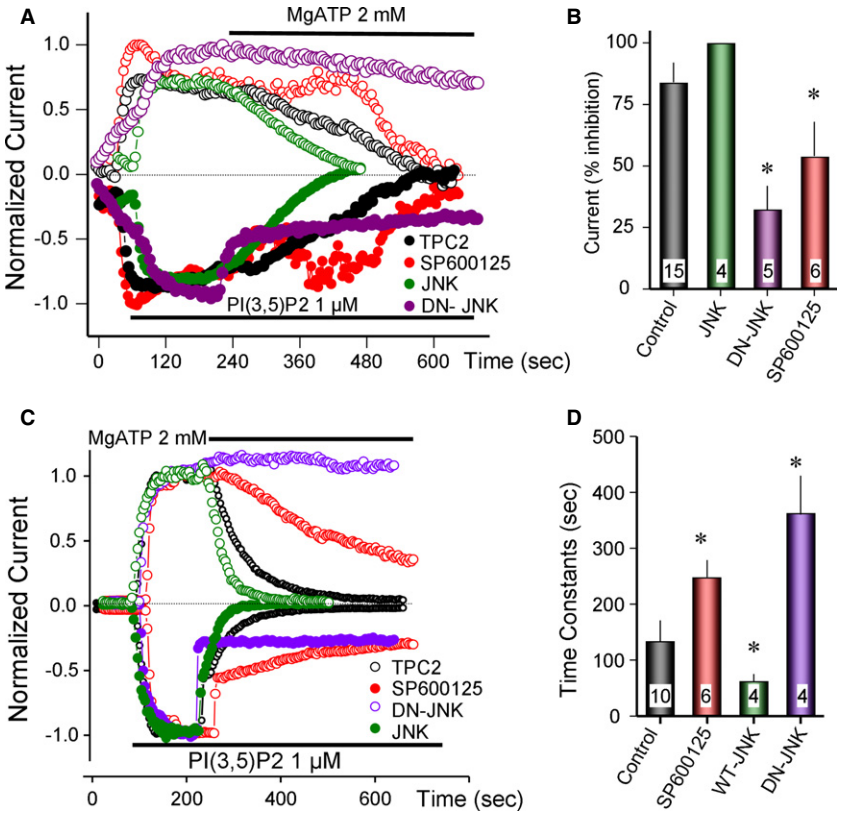

Figure 5. Regulation of TPC2 by JNK.

A, B All experiments are with TPC2 in lysosomes. The effect of JNK and DN-JNK was tested by transfecting the cells for 24 h with 1 µg/ml TPC2 and the kinases. The JNK inhibitor SP600125 was used at 0.4 µM (five times the K_i) and lysosomes were treated with the inhibitor for about 1–3 min before exposure to MgATP. The current was activated by 1 µM $PI(3,5)P_2$ and after maximal current was stable, the lysosomes were exposed to 2 mM MgATP. The outward current (filled symbols) was partially inhibited by the free Mg^{2+} in the MgATP mixture. The summary of current inhibition by MgATP is given in (B) and the results are given as the mean ±s.e.m. of the listed number of experiments. * denotes $P < 0.05$ relative to control. Note the inhibition of the MgATP effect by SP600125 and DN-JNK and its acceleration by JNK.

C, D Experiments similar to those in (A, B) using TPC2 in excised PM patches. The effect of MgATP was determined by calculating the time constants for inhibition by MgATP. The summary of current inhibition is given in (D) and the results are given as the mean ± s.e.m. of the listed number of experiments. * denotes $P < 0.05$ relative to control. Note the increased time constant by SP600125 and DN-JNK and reduced time constant by JNK.

Similarly, treating the cells with the JNK and P38 kinase inhibitors augmented the NAADP response (Supplementary Fig S6). Hence, the TPC2 current and NAADP-mediated Ca^{2+} release are similarly regulated by $PI(3,5)P_2$, Mg^{2+} and protein kinases.

Discussion

In addition to their canonical function in protein turnover, lysosomes play additional key roles in processes ranging from cellular energetics to cell death (Settembre *et al*, 2013). Lysosomal Ca^{2+} homeostasis is increasingly implicated in lysosomal function and dysfunction (Galione & Ruas, 2005; Patel *et al*, 2010; Patel & Muallem, 2011). In particular there has been much interest in the Ca^{2+} mobilizing messenger NAADP which releases Ca^{2+} from these acidic Ca^{2+} stores in a TPC-dependent manner (Brailoiu *et al*, 2009; Calcraft *et al*, 2009). Although multiple lines of evidence link NAADP-mediated Ca^{2+} release and the TPCs, the molecular mechanism underlying lysosomal Ca^{2+} release has proven controversial (Wang *et al*, 2012; Cang *et al*, 2013) and we know little of how this event is regulated.

Several discoveries in the present study, in particular inhibition of TPC2 by Mg^{2+} and multiple protein kinases, provide new insight into regulation of TPC2. We confirmed activation of TPC2 by $PI(3,5)P_2$ and its permeability to Na^+ (Fig 1). Notably, we found that in the absence of Mg^{2+}, TPC2 is readily activated by NAADP. The properties of the current activated by $PI(3,5)P_2$ and NAADP were highly similar. Thus, activation of the Na^+ current by NAADP could be observed only in lysosomes and PM patches obtained from cells transfected with TPC2 (Fig 3), and the current was partially inhibited by $Mg^{2+}{}_{lys}$ and strongly by $Mg^{2+}{}_{cyt}$ (Figs 1, 2 and 4, Supplementary Fig S2). The current activated by NAADP and $PI(3,5)P_2$ is selective for Na^+ over K^+ (Fig 4). In this respect, when reconstituted into bilayers, the TPC2 current activated by NAADP conducted K^+ (Pitt *et al*, 2010) or even showed high Ca^{2+} selectivity (Schieder *et al*, 2010). This suggests that the lipid environment may affect channel selectivity. Interestingly, activation by NAADP was more consistent when the current was recorded in lysosomes

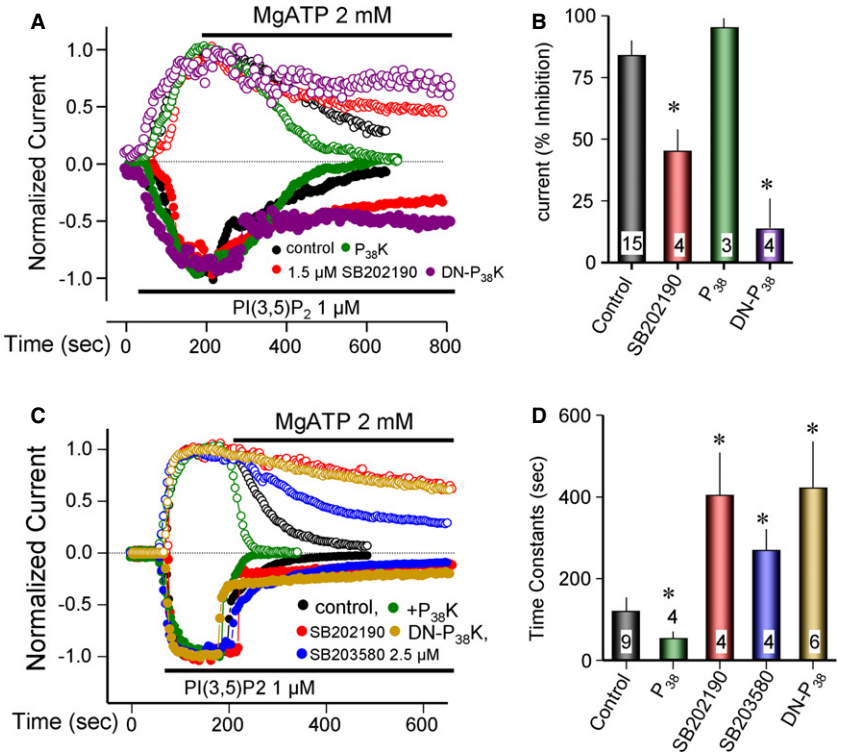

Figure 6. Regulation of TPC2 by the P38 MAP kinase.

A, B All experiments are with TPC2 in lysosomes. The transfection with P38 and DN-P38 and all experimental protocols are exactly as described in Fig 5 for JNK, except that the P38 inhibitor SB202190 was used at 1.5 μM (five times the K_i) and transfection was with 0.2 μg/ml P38 cDNA. After maximal current activation by 1 μM $PI(3,5)P_2$ lysosomes were treated with 2 mM MgATP. The summary of current inhibition by MgATP is given in (B) and the results are given as the mean ± s.e.m. of the listed number of experiments. * denotes $P < 0.05$ relative to control. Note the inhibition of the MgATP effect by SB202190 and DN-P38 and its acceleration by P38.

C, D The experiments are with TPC2 in excised PM patches. Expression of P38 markedly reduced the basal current. In four experiments there was a residual current, the extent of which is shown for one cell in the green trace of Supplementary Fig S5B. (C) shows the normalized currents. Inhibition of the residual current by MgATP was accelerated by P38. The DN-P38 strongly inhibited the effect of MgATP. Inhibition of the MgATP effect was also observed with two P38 inhibitors that act by different mechanisms, SB202190 and SB203580. The summary of current inhibition by MgATP is given in (D) and the results are given as the mean ± s.e.m. of the listed number of experiments. * denotes $P < 0.05$ relative to control.

compared to plasma membrane patches (Fig 3). This observation may relate to the finding that NAADP likely binds to small proteins that associate with TPCs (Lin-Moshier *et al*, 2011; Walseth *et al*, 2011). Redirecting TPC2 to the PM may therefore partially dissociate it from these regulatory proteins thus accounting for variability.

Another feature of our study is convergent regulation of TPC2 currents and NAADP-evoked Ca^{2+} release in intact cells by $PI(3,5)P_2$, Mg^{2+} and kinases. These data provide fresh evidence to support a role for TPCs in NAADP action. Interestingly, the response to NAADP in intact cells was augmented by increasing cellular $PI(3,5)P_2$ and inhibited by depletion of $PI(3,5)P_2$ (Fig 7). Hence, although $PI(3,5)P_2$ can fully activate TPC2 when applied to the cytoplasmic face of the channel under defined recording conditions, it is possible that in intact cells $PI(3,5)P_2$ has a permissive effect promoting activation of the channel by NAADP. Changes in endolysosomal $PI(3,5)P_2$ levels may thus modulate the size of the NAADP response. This topic needs further examination.

Considering the similarities in the regulation of NAADP-mediated Ca^{2+} release and the NAADP-activated TPC2 current, at present however, it is not easy to explain loss of TPCs current but retention of the NAADP-evoked Ca^{2+} responses in cells from TPC1/2 double knockout mice (Wang *et al*, 2012). Wang *et al* deleted only a portion of the N termini of the TPCs. Whether this resulted in complete deletion of the channels or simply redirected them to either the PM or the ER, given the presence of targeting information in these regions (Brailoiu *et al*, 2010; Churamani *et al*, 2013), remains to be established. In addition, Wang *et al* used a high concentration of NAADP-AM to characterize NAADP-evoked Ca^{2+} signals. Under these conditions, this compound may cause non-specific Ca^{2+} release from stores (Lu *et al*, 2013). In this respect, it is of note that responses to NAADP were eliminated in cells from an independent TPC2 knockout mouse line (Calcraft *et al*, 2009; Tugba Durlu-Kandilci *et al*, 2010).

Recent work suggests that lysosomes maintain high Na^+ levels (Wang *et al*, 2012) and that activation of TPC2 by $PI(3,5)P_2$ hyperpolarize the lysosomes (Cang *et al*, 2013), raising the question of the role of NAADP and TPC2 in Ca^{2+} release. Lysosomal hyperpolarization by NAADP is not likely to cause Ca^{2+} release since hyperpolarization should inhibit the release. TPC2 itself may mediate the Ca^{2+} release. Several studies have reported that TPCs are permeable

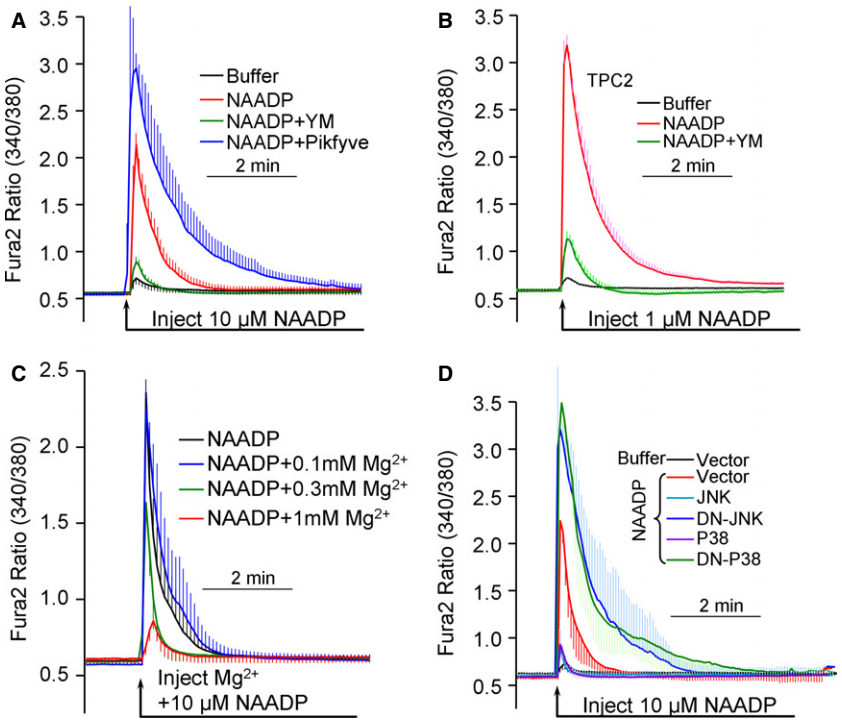

Figure 7. Regulation of NAADP-mediated Ca^{2+} release by $PI(3,5)P_2$, Mg^{2+}_{cyt}, JNK and P38.

A SKBR3 cells loaded with Fura2 were injected with intracellular-like buffer (black trace) or buffer containing 10 μM NAADP to result in a final concentration of about 100 nM (red trace). The cells were treated with 1 μM YM201636 for 2 h to deplete intracellular $PI(3,5)P_2$ (green trace) or transfected with Pikfyve for 24 h to increase intracellular $PI(3,5)P_2$ (blue trace) before injection with NAADP.

B Experiments as in (A), except that the SKBR3 cells were transfected with TPC2 and the injected buffer contained 1 μM NAADP, resulting in a final concentration of about 10 nM.

C Experiments were as in (A), except that the cells were injected with solution containing 10 μM NAADP and either 0 (control, black trace), 30 (blue trace), 100 (green trace) or 300 (red trace) mM $MgCl_2$ to yield a final concentrations of about 100 nM NAADP and 0.1, 0.3 or 1 mM free Mg^{2+}, respectively.

D SKBR3 cells were transfected with empty vector (black and red traces), JNK (Turquoise trace), DN-JNK (blue trace), P38 (purple trace) or DN-P38 (green trace) for 24 h before injection with buffer (black trace) of 10 μM NAADP (all other traces). In all experiments the traces are the mean ± s.e.m of 6–8 injections.

to Ca^{2+} (Brailoiu *et al*, 2010; Pitt *et al*, 2010; Rybalchenko *et al*, 2012), although the selectivity for Ca^{2+} relative to Na^+ appears to be low (~1:10) (Wang *et al*, 2012). However, the situation with TPC2 may be similar to the NMDA receptors, where both Na^+ and modest Ca^{2+} fluxes are physiologically relevant (Verkhratsky & Kirchhoff, 2007). In addition, we showed previously that NAADP could cause Ca^{2+} influx in cells expressing PM-targeted TPC2 in the face of 140 mM extracellular Na^+ (Brailoiu *et al*, 2010). The preliminary results in Supplementary Fig S7 show that $PI(3,5)P_2$ is also able to mediate Ca^{2+} influx through TPC2 and this influx is potentiated when extracellular Na^+ is lowered. Significantly, Ca^{2+} influx by activated TPC2 is comparable or higher than Ca^{2+} influx by PM-targeted TRPML1 which may release Ca^{2+} from the lysosomes (Dong *et al*, 2010). Hence, even limited permeability of TPC2 to Ca^{2+} may be sufficient to evoke global Ca^{2+} signals in an intact cell setting given intimate functional coupling between TPCs and ER Ca^{2+} channels. This is particularly relevant if such coupling occurs at microdomains (Kilpatrick *et al*, 2013). Secondary activation of other channels and/or transporters upon lysosomal hyperpolarization in response to NAADP however cannot be ruled out at this stage.

A key finding of the present work described in Figs 1–4 and Supplementary Fig S2 is the novel and complex regulation of TPC2 by Mg^{2+}. Both, Mg^{2+}_{lys} and Mg^{2+}_{cyt} affect TPC2 activity. The equal inhibition of the outward and inward currents by Mg^{2+}_{lys} suggests a general channel block that might be due to pore blockade, similar to the block of NMDA receptors by Mg^{2+} (Verkhratsky & Kirchhoff, 2007). Luminal lysosomal H^+ relieve inhibition of both inward and outward currents by Mg^{2+}_{lys}, probably by dissociating Mg^{2+}. These experiments also showed that channel conductance and selectivity appears to be unaffected by luminal pH, at least as low as pH 6.5 (Fig 2 and Supplementary Fig S1).

Arguably more interesting is regulation of TPC2 by Mg^{2+}_{cyt} that selectively inhibits outward Na^+ currents. The inhibition occurs with an apparent affinity of 0.06–0.13 mM. This is within the cytoplasmic free Mg^{2+} concentration which is 0.19–0.5 mM (Gunther, 2006). Hence small changes in Mg^{2+}_{cyt} markedly affect the activity of TPC2 and thus the lysosomal membrane potential. Decrease in Mg^{2+}_{cyt} will depolarize the lysosomal membrane potential to affect the transport of all electrogenic coupled and uncoupled transporters, including facilitation of Ca^{2+} release from the lysosomes. Thus, our findings indicate that a change in Mg^{2+}_{cyt} is a key regulator of lysosomal function. Several forms of cell stimulation that increase Ca^{2+} or cAMP cause an increase or a decrease in cytoplasmic Mg^{2+} that are associated with changes in anabolic and catabolic functions and

cell growth (Gunther, 2006). The finding of regulation of TPC2 by $Mg^{2+}{}_{cyt}$ may provide the link between the associated regulation of lysosomal and cellular functions.

The present work revealed that TPC2 is regulated by multiple protein kinases, thus implicating TPC2 in diverse cellular functions. The reported inhibition of TPC2 by mTORC1 linked TPC2 to energy metabolism (Cang *et al*, 2013). Although we could confirm inhibition of TPC2 by mTORC1, the inhibition was modest (Supplementary Fig S2), leading us to identify prominent regulation by JNK and P38 (Figs 5 and 6). These kinases play central roles in cell proliferation, differentiation and cancer. JNK and P38 are structurally and enzymatically similar (Johnson & Lapadat, 2002) that may account for their similar regulatory effects on TPC2, although they have largely different cellular functions. The most prominent function of P38 linked to lysosomes is its role in inflammation and associated autophagy (Cuenda & Rousseau, 2007). Many cell stressors that induce apoptosis do so by acting on P38 (Wagner & Nebreda, 2009). The main function of the JNKs is in cell proliferation through transcriptional activation (Jaeschke *et al*, 2006). In addition, JNKs also regulate autophagy through phosphorylation of BCL-2 to release it from Beclin 1 to control Beclin 1 transcription (Mehrpour *et al*, 2010). It is thus possible that lysosomal P38 and JNK inhibit TPC2 to control lysosomal membrane potential and Ca^{2+} release (see Fig 7) to inhibit autophagy. Indeed, NAADP/TPC2 has recently been shown to regulate autophagy (Pereira *et al*, 2011; Lu *et al*, 2013).

In summary, the present work revealed novel regulatory modalities of the endolysosomal channel TPC2 by Mg^{2+} and multiple protein kinases. These forms of regulation should have profound effect on the function of the lysosome. The protein kinases appear to inhibit the function of TPC2 on a time scale of many minutes and thus can set the steady-state function of the lysosomes in response to inputs related to inflammatory cell stressors (P38), transcriptional demand (JNK), induction of apoptosis (P38 and JNK) or nutrient supply (mTORC1). Regulation by Mg^{2+} is on a sub-seconds time scale and is most suited to control the lysosomal membrane potential and thus its ionic fluxes and content. Further studies are required to determine how each of the regulatory modalities comes into play during various cellular demands for lysosomal function.

Materials and Methods

Reagents and solutions

The GFP-TPC2 clone was described elsewhere (Yamaguchi *et al*, 2011) and GFP-TPC2-$L^{11}L^{12}$/AA mutant was generated by site directed mutagenesis. Several clones were obtained from Addgene (cat no.) mTORC1 (26603), DN-mTORC1 (26605), JNK (19731) DN-JNK (19730), P38 (20355), DN-P38 (20356). The Pikfyve clone was from Open Biosystems (MHS1010-202696678). The MAP kinase inhibitors kit was from Tocris. The $PI(3,5)P_2$ kinase inhibitor YM201636 and $PI(3,5)P_2$ were from Cayman Chemical. NAADP and vacuolin were from Sigma. The $PI(3,5)P_2$ carrier and lipid soluble $PI(3,5)P_2$ kit were from Echelon Biosciences. For recording lysosomal current the standard pipette (luminal) solution contained (mM) 140 NaCl, 5 KCl, 10 HEPES (pH 7.4 with NaOH) and the standard bath (cytoplasmic) solution contained 140 NaCl, 5 KCl or 140 KCl, 10 HEPES (pH 7.4 with NaOH or KOH). As needed, Mg^{2+} was added to either or to both solutions. The same solutions were used to record current in excised plasma membrane (PM) patches, except that where indicated the pipette (luminal) solution was adjusted to pH 7.4 or 6.5. The whole-cell current was recorded with pipette solution containing (mM) either 140 Na^+-Gluconate or Cs^+-$MeSO_4$, 10 NaCl or CsCl, 10 HEPES (pH 7.4 with NaOH or CsOH), 0.39 Ca^{2+}, 1 EGTA (final free Ca^{2+} of 100 nM) and with or without 1 Mg^{2+} and with or without 200 μM $PI(3,5)P_2$ or 1 μM NAADP. The bath solution contained 140 Na^+-Gluconate or $NMDG^+$-Gluconate, 5 KCl, 10 HEPES (pH 7.4 with NaOH or Tris base).

Cells

HEK293T and COS-7 cells were maintained in DMEM and 10% fetal bovine serum supplemented with penicillin (100 units/ml)/streptomycin (100 μg/ml), and the cells were maintained in a water-saturated 5% CO_2, 95% air atmosphere. Cells were transiently transfected with GFP-TPC2/GFP-TPC2-$L^{11}L^{12}$/AA with and without the kinases using Lipofectamine 2000 and were used 24–36 h post-transfection. In experiments with cells transfected with P38 or high level of JNK kinases that strongly inhibited the basal TPC2 activity, the cells were also treated with the respective kinase inhibitors for 2 h before current measurement to demonstrate reversal of the inhibition. Lysosomes were isolated from COS-7 cells transfected with GFP-TPC2 and the indicated kinases. Lysosomes were liberated mechanically and patched within 1–2 min of release. Plasma membrane patches were excised from HEK cells transfected with GFP-TPC2 and the kinases. SKBR3 were maintained in McCoy's 5A modified media and 10% fetal bovine serum. Cells were transiently transfected using Turbofectin 8. Cells were used 48–72 h after transfection.

Current recording

Whole lysosomal current recordings were performed using a modified patch clamp method (Dong *et al*, 2010). Transfected COS-7 cells were released and replated on Petri dishes and incubated with culture media for 1 h to allow attachment. Then the cells were treated with 1 μM vacuolin-1, for 1–2 h. Patch pipettes had a resistance of 5–8 MΩ when filled with the pipette solution. Enlarged lysosomes were released by quickly pressing patch pipettes against the cell and pulling back. The enlarged lysosomes were identified by monitoring GFP fluorescence. After formation of a GΩ seal, capacitance transients were compensated by Axopatch 200B patch clamp amplifier. For breaking into the lysosomes, quick voltage steps of positive 350 mV were applied. The whole lysosomal configuration was confirmed by reappearance of the capacitance transient. The current was recorded by 400-ms rapid alterations of membrane potential (RAMP) from −150 to +120 mV from a holding potential of 0 mV at 4 s intervals. The whole-lysosomal currents were filtered at 1 kHz with an internal four-pole Bessel filter, sampled at 5 kHz, and stored directly to a hard drive by Digidata 1322. Whole-cell current was recorded from transfected HEK293T cells using standard technique. Patch pipettes were heat-polished and had a resistance of 3–5 MΩ when filled with the pipette solution. Current was measured with an Axopatch 200B patch clamp amplifier that was controlled by pCLAMP9 software to allow the delivery of

voltage-step protocols with concomitant digitization. The currents were sampled at 5 kHz and filtered at 1 kHz. Currents were obtained by voltage ramps with command voltage from −150 to +120 mV over 400 or 200 ms every 4 s from a holding potential of 0 mV. Inside-out patches were excised from HEK cells with pipettes having resistance of 3–5 MΩ. After formation of a GΩ seals patches were pulled quickly away from the cell. The current was recorded by 400-ms RAMPs from −150 to +120 mV from a holding potential of 0 mV at 4 s intervals.

Ca^{2+} measurements

For measurement of Ca^{2+} influx in HEK cells transfected with GFP-TPC2-$L^{11}L^{12}$/AA or mCherry-TRPML1(ΔNΔC), the cells were incubated with 1 μM $PI(3,5)P_2$, 0.3 μM carrier or $PI(3,5)P_2$ and carrier for 1 h at 37°C in Ca^{2+}-free DMEM solution containing 0.2 mM EGTA. During the last 20 min the cell were loaded with Fura2 and Ca^{2+} was measured as the 340/380 ratio. External Na^+ was reduced by replacing NaCl with NMDG-Cl. Ca^{2+} measurement in SKBR3 cells was as before (Brailoiu *et al*, 2009). Fura2 loaded cells on coverslips were mounted in an open chamber in a Nikon Eclipse TiE microscope equipped with a Perfect Focus System and a Photometrics CoolSnap HQ2 CCD camera. TPC2-transfected cells were identified by the YFP fluorescence and when TPC2 was not expressed, the P38 and JNK kinases and their mutants were co-expressed with YFP to identify the transfected cells. Fura2 fluorescence was acquired at a frequency of 0.25 Hz and images were analyzed using NIS-Elements AR software. Injections were as before (Brailoiu *et al*, 2009). Pipettes were back-filled with an intracellular solution composed of (mM) 110 KCl, 10 NaCl, and 20 HEPES (pH 7.2) and with or without NAADP and Mg^{2+}. The cells to be injected were Z scanned and the cellular volume was calculated using Nikon NIS-Elements AR software prior to injection. The injection time was 0.4 s at 60 h Pascal with a compensation pressure of 20 h Pa to maintain the microinjected volume to <1% of cell volume.

Statistics

All experiments were repeated at least three times and the results are given as means ± s.e.m. Differences between the groups were analyzed for statistical significance by un-paired Student's *t*-test. $P < 0.05$ or better was considered statistically significant.

Supplementary information for this article is available online: http://emboj.embopress.org

Acknowledgements

This work was supported in part by National Institutes of Health Grants HL090804 to E.B. and by NIH/NIDCR intramural grant DE000735-03 to S.M.

Author contributions

AJ, MA and EB performed and analyzed the experiments, SP provided essential material, EB and SM designed and directed the studies, SM drafted the manuscript with input from all authors.

Conflict of interest

All authors declare that they have no conflict of interests.

References

Aarhus R, Dickey DM, Graeff RM, Gee KR, Walseth TF, Lee HC (1996) Activation and inactivation of Ca^2+ release by NAADP+. *J Biol Chem* 271: 8513–8516

Bertl A, Blumwald E, Coronado R, Eisenberg R, Findlay G, Gradmann D, Hille B, Kohler K, Kolb HA, MacRobbie E, Meinsser G, Miller C, Neher E, Palade P, Pantoja O, Sanders D, Schroeder J, Slayman C, Spanswick R, Walker A, *et al* (1992) Electrical measurements on endomembranes. *Science* 258: 873–874

Brailoiu E, Churamani D, Cai X, Schrlau MG, Brailoiu GC, Gao X, Hooper R, Boulware MJ, Dun NJ, Marchant JS, Patel S (2009) Essential requirement for two-pore channel 1 in NAADP-mediated calcium signaling. *J Cell Biol* 186: 201–209

Brailoiu E, Rahman T, Churamani D, Prole DL, Brailoiu GC, Hooper R, Taylor CW, Patel S (2010) An NAADP-gated two-pore channel targeted to the plasma membrane uncouples triggering from amplifying Ca^2+ signals. *J Biol Chem* 285: 38511–38516

Calcraft PJ, Ruas M, Pan Z, Cheng X, Arredouani A, Hao X, Tang J, Rietdorf K, Teboul L, Chuang KT, Lin P, Xiao R, Wang C, Zhu Y, Lin Y, Wyatt CN, Parrington J, Ma J, Evans AM, Galione A *et al* (2009) NAADP mobilizes calcium from acidic organelles through two-pore channels. *Nature* 459: 596–600

Cang C, Zhou Y, Navarro B, Seo YJ, Aranda K, Shi L, Battaglia-Hsu S, Nissim I, Clapham DE, Ren D (2013) mTOR regulates lysosomal ATP-sensitive two-pore Na(+) channels to adapt to metabolic state. *Cell* 152: 778–790

Churamani D, Hooper R, Rahman T, Brailoiu E, Patel S (2013) The N-terminal region of two-pore channel 1 regulates trafficking and activation by NAADP. *Biochem J* 453: 147–151

Churchill GC, Okada Y, Thomas JM, Genazzani AA, Patel S, Galione A (2002) NAADP mobilizes Ca(2+) from reserve granules, lysosome-related organelles, in sea urchin eggs. *Cell* 111: 703–708

Clapham DE (2007) Calcium signaling. *Cell* 131: 1047–1058

Cuenda A, Rousseau S (2007) p38 MAP-kinases pathway regulation, function and role in human diseases. *Biochim Biophys Acta* 1773: 1358–1375

Dionisio N, Albarran L, Lopez JJ, Berna-Erro A, Salido GM, Bobe R, Rosado JA (2011) Acidic NAADP-releasable Ca(2+) compartments in the megakaryoblastic cell line MEG01. *Biochim Biophys Acta* 1813: 1483–1494

Dong XP, Shen D, Wang X, Dawson T, Li X, Zhang Q, Cheng X, Zhang Y, Weisman LS, Delling M, Xu H (2010) PI(3,5)P(2) controls membrane trafficking by direct activation of mucolipin Ca(2+) release channels in the endolysosome. *Nat Commun* 1: 38

Galione A, Ruas M (2005) NAADP receptors. *Cell Calcium* 38: 273–280

Genazzani AA, Empson RM, Galione A (1996) Unique inactivation properties of NAADP-sensitive Ca2+ release. *J Biol Chem* 271: 11599–11602

Gunther T (2006) Concentration, compartmentation and metabolic function of intracellular free Mg2+. *Magnes Res* 19: 225–236

Guse AH, Lee HC (2008) NAADP: a universal Ca2+ trigger. *Sci Signal* 1: re10

Ho CY, Alghamdi TA, Botelho RJ (2012) Phosphatidylinositol-3,5-bisphosphate: no longer the poor PI *Traffic* 2: 1–3

Jaeschke A, Karasarides M, Ventura JJ, Ehrhardt A, Zhang C, Flavell RA, Shokat KM, Davis RJ (2006) JNK2 is a positive regulator of the cJun transcription factor. *Mol Cell* 23: 899–911

Jewell JL, Russell RC, Guan KL (2013) Amino acid signalling upstream of mTOR. *Nat Rev Mol Cell Biol* 14: 133–139

Johnson GL, Lapadat R (2002) Mitogen-activated protein kinase pathways mediated by ERK, JNK, and p38 protein kinases. *Science* 298: 1911 – 1912

Kilpatrick BS, Eden ER, Schapira AH, Futter CE, Patel S (2013) Direct mobilisation of lysosomal Ca2+ triggers complex Ca2+ signals. *J Cell Sci* 126: 60 – 66

Kinnear NP, Boittin FX, Thomas JM, Galione A, Evans AM (2004) Lysosome-sarcoplasmic reticulum junctions. A trigger zone for calcium signaling by nicotinic acid adenine dinucleotide phosphate and endothelin-1. *J Biol Chem* 279: 54319 – 54326

Kiselyov K, Chen J, Rbaibi Y, Oberdick D, Tjon-Kon-Sang S, Shcheynikov N, Muallem S, Soyombo A (2005) TRP-ML1 is a lysosomal monovalent cation channel that undergoes proteolytic cleavage. *J Biol Chem* 280: 43218 – 43223

Kiselyov K, Wang X, Shin DM, Zang W, Muallem S (2006) Calcium signaling complexes in microdomains of polarized secretory cells. *Cell Calcium* 40: 451 – 459

Kiselyov KK, Ahuja M, Rybalchenko V, Patel S, Muallem S (2012) The intracellular Ca(2)(+) channels of membrane traffic. *Channels* 6: 344 – 351

Kroemer G, Marino G, Levine B (2010) Autophagy and the integrated stress response. *Mol Cell* 40: 280 – 293

Lee HC, Aarhus R (1995) A derivative of NADP mobilizes calcium stores insensitive to inositol trisphosphate and cyclic ADP-ribose. *J Biol Chem* 270: 2152 – 2157

Lin-Moshier Y, Walseth TF, Churamani D, Davidson SM, Slama JT, Hooper R, Brailoiu E, Patel S, Marchant JS (2011) Photoaffinity labeling of nicotinic acid adenine dinucleotide phosphate (NAADP) targets in mammalian cells. *J Biol Chem* 287: 2296 – 2307

Lu YY, Hao BX, Graeff R, Wong CW, Wu WT, Yue J (2013) TPC2 signaling inhibits autophagosomal-lysosomal fusion by alkalizing lysosomal pH. *J Biol Chem* 288: 24247 – 24263

Mehrpour M, Esclatine A, Beau I, Codogno P (2010) Overview of macroautophagy regulation in mammalian cells. *Cell Res* 20: 748 – 762

Morgan AJ, Davis LC, Wagner SK, Lewis AM, Parrington J, Churchill GC, Galione A (2013) Bidirectional Ca(2)(+) signaling occurs between the endoplasmic reticulum and acidic organelles. *J Cell Biol* 200: 789 – 805

Morgan AJ, Platt FM, Lloyd-Evans E, Galione A (2011) Molecular mechanisms of endolysosomal Ca2+ signalling in health and disease. *Biochem J* 439: 349 – 374

Patel S, Marchant JS, Brailoiu E (2010) Two-pore channels: regulation by NAADP and customized roles in triggering calcium signals. *Cell Calcium* 47: 480 – 490

Patel S, Muallem S (2011) Acidic Ca(2+) stores come to the fore. *Cell Calcium* 50: 109 – 112

Pereira GJ, Hirata H, Fimia GM, do Carmo LG, Bincoletto C, Han SW, Stilhano RS, Ureshino RP, Bloor-Young D, Churchill G, Piacentini M, Patel S, Smaili SS (2011) Nicotinic acid adenine dinucleotide phosphate (NAADP) regulates autophagy in cultured astrocytes. *J Biol Chem* 286: 27875 – 27881

Pitt SJ, Funnell TM, Sitsapesan M, Venturi E, Rietdorf K, Ruas M, Ganesan A, Gosain R, Churchill GC, Zhu MX, Parrington J, Galione A, Sitsapesan R (2010) TPC2 is a novel NAADP-sensitive Ca2+ release channel, operating as a dual sensor of luminal pH and Ca2+. *J Biol Chem* 285: 35039 – 35046

Pryor PR, Reimann F, Gribble FM, Luzio JP (2006) Mucolipin-1 is a lysosomal membrane protein required for intracellular lactosylceramide traffic. *Traffic* 7: 1388 – 1398

Rybalchenko V, Ahuja M, Coblentz J, Churamani D, Patel S, Kiselyov K, Muallem S (2012) Membrane potential regulates nicotinic acid adenine dinucleotide phosphate (NAADP) dependence of the pH- and Ca2+-sensitive organellar two-pore channel TPC1. *J Biol Chem* 287: 20407 – 20416

Saftig P, Klumperman J (2009) Lysosome biogenesis and lysosomal membrane proteins: trafficking meets function. *Nat Rev Mol Cell Biol* 10: 623 – 635

Schieder M, Rotzer K, Bruggemann A, Biel M, Wahl-Schott CA (2010) Characterization of two-pore channel 2 (TPCN2)-mediated Ca2+ currents in isolated lysosomes. *J Biol Chem* 285: 21219 – 21222

Settembre C, Fraldi A, Medina DL, Ballabio A (2013) Signals from the lysosome: a control centre for cellular clearance and energy metabolism. *Nat Rev Mol Cell Biol* 14: 283 – 296

Shen D, Wang X, Li X, Zhang X, Yao Z, Dibble S, Dong XP, Yu T, Lieberman AP, Showalter HD, Xu H (2012) Lipid storage disorders block lysosomal trafficking by inhibiting a TRP channel and lysosomal calcium release. *Nat Commun* 3: 731

Tugba Durlu-Kandilci N, Ruas M, Chuang KT, Brading A, Parrington J, Galione A (2010) TPC2 proteins mediate nicotinic acid adenine dinucleotide phosphate (NAADP)- and agonist-evoked contractions of smooth muscle. *J Biol Chem* 285: 24925 – 24932

Verkhratsky A, Kirchhoff F (2007) NMDA receptors in glia. *Neuroscientist* 13: 28 – 37

Wagner EF, Nebreda AR (2009) Signal integration by JNK and p38 MAPK pathways in cancer development. *Nat Rev Cancer* 9: 537 – 549

Walseth TF, Lin-Moshier Y, Jain P, Ruas M, Parrington J, Galione A, Marchant JS, Slama JT (2011) Photoaffinity labeling of high affinity nicotinic acid adenine dinucleotide 2′-phosphate (NAADP) proteins in sea urchin egg. *J Biol Chem* 287: 2308 – 2315

Wang X, Zhang X, Dong XP, Samie M, Li X, Cheng X, Goschka A, Shen D, Zhou Y, Harlow J, Zhu MX, Clapham DE, Ren D, Xu H (2012) TPC proteins are phosphoinositide- activated sodium-selective ion channels in endosomes and lysosomes. *Cell* 151: 372 – 383

Yamaguchi S, Jha A, Li Q, Soyombo AA, Dickinson GD, Churamani D, Brailoiu E, Patel S, Muallem S (2011) Transient receptor potential mucolipin 1 (TRPML1) and two-pore channels are functionally independent organellar ion channels. *J Biol Chem* 286: 22934 – 22942

Zhang F, Xu M, Han WQ, Li PL (2011) Reconstitution of lysosomal NAADP-TRP-ML1 signaling pathway and its function in TRP-ML1(−/−) cells. *Am J Physiol Cell Physiol* 301: C421 – C430

Zong X, Schieder M, Cuny H, Fenske S, Gruner C, Rotzer K, Griesbeck O, Harz H, Biel M, Wahl-Schott C (2009) The two-pore channel TPCN2 mediates NAADP-dependent Ca(2+)-release from lysosomal stores. *Pflugers Arch* 458: 891 – 899